

Interacting ferromagnetic nanoparticles in discontinuous $\text{Co}_{80}\text{Fe}_{20}/\text{Al}_2\text{O}_3$ multilayers: From superspin glass to reentrant superferromagnetism

W. Kleemann, O. Petravic, and Ch. Binek

Laboratorium für Angewandte Physik, Gerhard-Mercator-Universität, D-47048 Duisburg, Germany

G. N. Kakazei, Yu. G. Pogorelov, and J. B. Sousa

IFIMUP, Departamento de Física, Universidade de Porto, 4169-007 Porto, Portugal

S. Cardoso and P. P. Freitas

INESC, Rua Alves Redol 9-1, 1000, Lisbon, Portugal

(Received 5 December 2000; published 12 March 2001)

Dipolar superferromagnetism with reentrant low-temperature superspin glass behavior is observed on a randomly distributed ferromagnetic nanoparticle systems in discontinuous metal-insulator multilayers $[\text{Co}_{80}\text{Fe}_{20}(t)/\text{Al}_2\text{O}_3(3\text{ nm})]_{10}$ with nominal thickness $1.1 \leq t \leq 1.3$ nm by use of ac susceptometry and dc magnetometry. At $t = 1.0$ nm, superspin glass-like freezing is evidenced by the criticality of dynamic and nonlinear susceptibilities.

DOI: 10.1103/PhysRevB.63.134423

PACS number(s): 75.10.Nr, 75.30.Kz, 75.40.Gb

I. INTRODUCTION

Dipolar interactions in ferromagnetic (FM) single domain nanoparticle assemblies have recently become a matter of intense research.¹ It is now widely accepted that a crossover from pure Néel-Brown-type² *superparamagnetic* (SPM) to *superspin glass* (SSG) behavior takes place at low enough temperature (T) for three-dimensional (3D) randomly distributed nanoparticle systems for high enough density and sufficiently narrow size distribution.^{3,4} However, transitions into *superferromagnetic* (SFM) long-range order have hitherto been observed only in one- (1D) and two-dimensional (2D) self-organized⁵ or regularly structured⁶ arrays of FM nanoparticles. While in most cases^{5,6} dipolar interactions seem to prevail, exchange coupling of the supermoments was also conjectured in distinct cases.⁷ The question arises, why SPM-to-SFM transitions have never been observed in $D = 3$ nanoparticle systems even in the limit of nearly close packing, i.e., at a diameter-to-distance ratio $r \cong 1$.⁴ Indeed, coupling of point dipoles both in 2D and 3D systems was predicted to form antiferromagnetic domain states.⁸ However, it was recently shown⁹ that dipolar stray fields between *finite-size* granules (superspines) can produce FM coupling (henceforth denoted as “*superexchange*”) and that this “*superexchange*” can give rise to SFM order in 2D granular systems above some critical value, $r_{\text{cr}} \approx 0.87$, but is less probable in the 3D case.

Only recently we have discovered superferromagnetism in disordered nanoparticle systems.¹⁰ It has been observed in discontinuous metal-insulator multilayers (DMIM)^{11,12} of $[\text{Co}_{80}\text{Fe}_{20}(t)/\text{Al}_2\text{O}_3(3\text{ nm})]_{10}$ at high enough CoFe particle densities. Varying t at a fixed interlayer distance of 3 nm effectively changes the in-plane ratio r . Thus, at $r > r_{\text{cr}}$, one can expect 2D-like SFM order, essentially dominated by the above “*superexchange*.” At $r < r_{\text{cr}}$, however, 3D coupling dominates, which leads to a SSG state at low enough T .

Peculiarly, in the case $r > r_{\text{cr}}$ —as a tribute to intrinsic

randomness—reentrance into a SSG phase is encountered at low temperatures similarly as in amorphous¹³ and nanocrystalline¹⁴ FM materials. It is argued in this case that SSG and SFM ordering takes place on different percolating clusters, thus establishing the coexistence of two phases. At low CoFe concentration, the SFM becomes unstable and only the SSG phase survives.

DMIM’s consist of layers with closely spaced FM granules intercalated between insulating spacer layers. They are interesting for tunneling magnetoresistive (MR) applications with room temperature (RT) MR ratios up to 7%.^{11,12} In the CoFe/Al₂O₃ system, two different “*percolation*” limits were found from transport and magnetic properties, respectively. While the change from insulating to metallic behavior occurs above the percolation threshold, $t \approx 1.8$ nm,¹² SFM long-range order as indicated by hysteresis appears at RT for $t > t^* = 1.3$ nm.¹⁵

II. EXPERIMENTAL PROCEDURE

In our present investigation, we employed ac susceptibility and dc magnetization techniques by use of a superconducting quantum interference device magnetometer (Quantum Design MPMS-5S) at temperatures $4 \leq T \leq 300$ K, magnetic fields $|\mu_0 H| \leq 5$ T and frequencies $10^{-3} \leq f \leq 500$ Hz. The CoFe/Al₂O₃ DMIM’s were prepared by Xe ion beam sputtering on glass substrates.^{12,15} While the Al₂O₃ layer thickness was fixed at 3.0 nm, the nominal thickness of the CoFe layers was varied between $1.0 \leq t \leq 1.3$ nm.

Figure 1(a) shows a schematic sketch of the cross section indicating the glass substrate, the Al₂O₃ layers of fixed thickness 3 nm and the CoFe layers of thickness t , which disassemble into quasispherical nanoparticles owing to nonwetting conditions. A high-resolution transmission top view micrograph on a CoFe ($t = 1.3$ nm)/Al₂O₃ ($t = 3$ nm) bilayer¹⁵ is shown in Fig. 1(b) where solid dark circles indicate the CoFe nanoparticles embedded in a gray-scaled Al₂O₃ environment. The granules turn out to be nearly

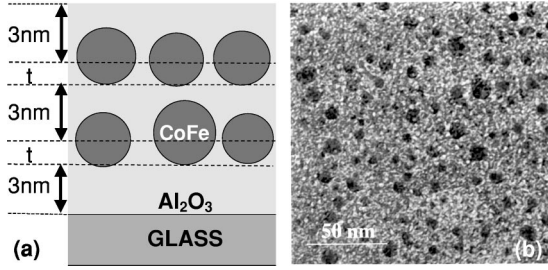


FIG. 1. (a) Schematic cross section of a DMIM consisting of substrate, Al_2O_3 layers (thickness 3 nm) and CoFe layers (t) forming quasispherical nanoparticles, and (b) transmission top view electron micrograph of a CoFe ($t = 1.3$ nm)/ Al_2O_3 ($t = 3$ nm) bilayer, (Ref. 15) where dark circles indicate CoFe nanoparticles embedded into gray-scaled Al_2O_3 .

spherical having an average diameter $d \approx 3$ nm within a log-normal distribution width of $\sigma \approx 2.7$.¹⁵ In accordance with the observed transport properties¹² heterogeneous nucleation has to be assumed in these DMIM's. Hence, the granule size increases linearly with CoFe layer thickness t while their average clearance monotonically decreases until reaching 3D percolation at $t \approx 1.8$ nm, where tunneling is masked by conventional ohmic conductivity. On the other hand, equidistance between the granules along all spatial directions is expected to occur at $t \approx 0.9$ nm.

III. EXPERIMENTAL RESULTS AND DISCUSSION

Susceptibility data taken at an ac amplitude δ ($\mu_0 H$) = 0.4 mT in a virtually vanishing external field (see below) are shown in Fig. 2 for four different DMIM's at various frequencies, $0.1 \leq f \leq 100$ Hz. For the $t = 1.0$ nm sample (a) $\chi'(f, T)$ and $\chi''(f, T)$ are similar to data observed previously on frozen FeC ferrofluids.³ While sizeable dispersion characterizes the range $40 \leq T \leq 80$ K, nondispersive Curie-Weiss (CW)-type decay of $\chi'(f, T)$ with an extrapolated FM Curie temperature $\Theta \approx 58$ K is encountered at $T > 80$ K [see inverse susceptibility curves for $f = 0.1$ Hz and CW plot best fitted within $200 \leq T \leq 300$ K in Fig. 2(a)].

Convergence of the peak temperatures T_m of $\chi'(f, T)$ towards a finite glass temperature T_g at low- f values is shown in Fig. 3(a) in a double-logarithmic plot of $\tau = (2\pi f)^{-1}$ vs $T_m/T_g - 1$. In order to minimize effects due to nonlinear response (see below) the data (not shown) were recorded at a very small field amplitude, δ ($\mu_0 H$) = 0.05 mT, and frequencies $0.01 \leq f \leq 1$ Hz. A best fit of the data to the power law of critical dynamics,³ $\tau = \tau_0 (T_m/T_g - 1)^{-z\nu}$, is obtained with $T_g = (47.1 \pm 5.3)$ K, $\tau_0 = (6.7 \pm 0.4) \cdot 10^{-7}$ s, and $z\nu = 10.0 \pm 3.6$. Similar results, albeit with shorter τ_0 values, were obtained on FeC and γ - Fe_2O_3 nanoparticle systems.^{3,4} While the value of $z\nu$ agrees with that predicted for 3D spin glasses,¹⁶ the large ‘‘spin-flip’’ time τ_0 accounts for the cluster nature of the ‘‘superspins.’’^{3,17}

Nonlinear susceptibility studies corroborate the above conjectured SSG nature of the DMIM system with $t = 1.0$ nm. To this end, magnetization curves M vs H were recorded after zero-field cooling (ZFC) from $T = 300$ K at

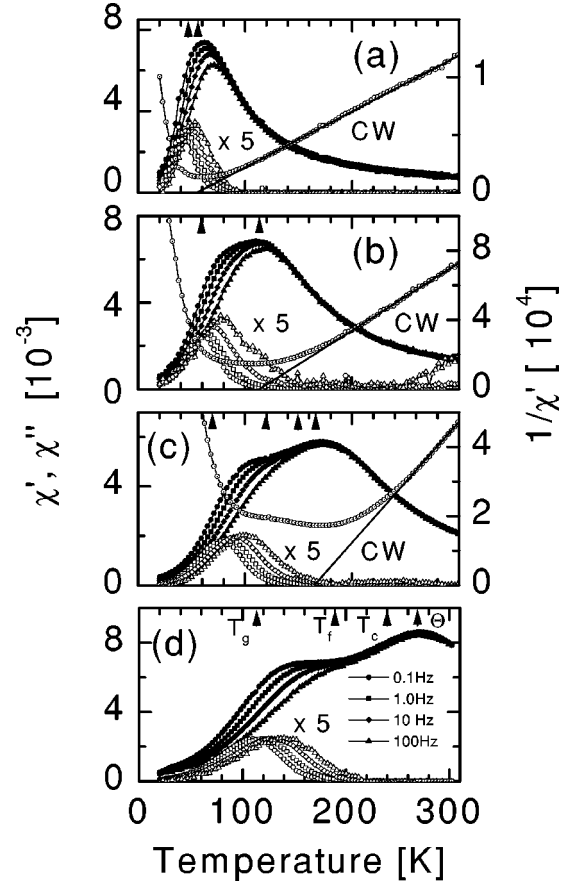


FIG. 2. $\chi'(f, T)$ and $\chi''(f, T)$ vs T of CoFe/ Al_2O_3 DMIMs with $t = 1.0$ (a), 1.1 (b), 1.2 (c), and 1.3 nm (d) measured at frequencies $0.1 \leq f \leq 100$ Hz. Note the magnification factor ($5 \times$) applicable to all χ'' data. Inverse curves $\chi^{-1}(f = 0.1 \text{ Hz}, T)$ with best-fitted Curie-Weiss (CW) lines define the mean-field transition temperatures, Θ , as marked by arrowheads together with T_g , T_f , and T_c (c and d only), where $T_g < T_f < T_c < \Theta$ (see text).

temperatures $55 \leq T \leq 65$ K in fields $-0.02 \leq \mu_0 H \leq 0.6$ mT in steps of 0.01 mT. In order to warrant thermal equilibrium, the critical slowing down has been overcome by isothermal waiting times between data points, $t_w = 100$ and 500 s at $T > 60$ K and ≤ 60 K, respectively. The data were fitted to a polynomial, $M = \chi_1 H - \chi_3 H^3 + \chi_5 H^5$, where χ_3 is expected to diverge at T_g in case of a collective spin-glasslike phase transition.¹² The results are plotted in Fig. 3(b) together with a best-fitted power law, $\chi_3 = \chi_3^0 (T/T_g - 1)^{-\gamma}$ revealing $T_g = (50.7 \pm 2.3)$ K, $\gamma = 1.36 \pm 0.53$ and $\chi_3^0 = (2.5 \pm 1.3) \cdot 10^{-9}$ (m/A)². Within errors, T_g agrees with the value obtained from dynamic scaling (see above). The critical exponent γ is smaller than that observed on spin glasses ($\gamma \approx 4$).¹⁸ This seems to hint either at a proximity to mean-field behavior ($\gamma = 1$) (Ref. 13) owing to the long-range nature of the dipolar interaction, or at spurious blocking processes of large particles within the relatively broad log-normal particle size distribution ($\sigma \approx 2.7$ for $t = 1.3$ nm) (Ref. 15) in our samples.

At higher nominal thickness, $t \geq 1.1$ nm, a dispersionless background appears in addition to the response curves of the

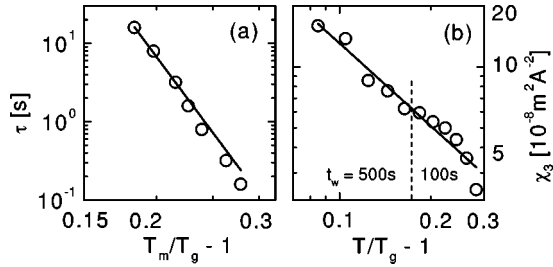


FIG. 3. Double-logarithmic plots of (a) $\tau = (2\pi f)^{-1}$ vs $T_m/T_g - 1$ and (b) χ_3 vs $T/T_g - 1$ (obtained after waiting times t_w as indicated) for the DMIM with $t = 1.0$ nm, where $T_g = (47.1 \pm 5.3)$ and (50.7 ± 2.3) K, respectively, from best fits to power laws (straight lines).

polydispersive glassy subsystem at higher temperatures [Figs. 2(b)–2(d)]. CW-type high- T tails are encountered with FM mean-field Curie temperatures $\Theta(t) \approx 114, 165,$ and 270 K for $t = 1.1, 1.2,$ and 1.3 nm, respectively [see $1/\chi$ curves for $f = 0.1$ Hz and CW plots best fitted above 240 K in Figs. 2(b)–2(c)]. Below we shall attribute the background curves to the prevalence of “superexchange”⁹ over purely dipolar coupling⁸ in the “percolating” cluster system. It behaves like a *superferromagnet* with finite in-plane anisotropy, which causes the susceptibility to increase upon heating towards the SFM ordering temperature, $T_c < \Theta$. Notably, the dispersionless part of $\chi'(f, T)$ is unrelated to the loss function, $\chi''(f, T)$. This is at variance with a recently reported¹⁹ $\chi'(f, T)$ curve in a 3D granular system exhibiting two peaks. Since both of them were accompanied by sizeable losses, their assignment¹⁹ to a SFM-SSG transition sequence appears doubtful. It should be noticed that the data shown in Fig. 2 were recorded at a weak bias field of $\mu_0 H \approx -0.6$ mT due to some remanence of our superconducting solenoid. As will be reported elsewhere,²⁰ this does not invalidate our inferences on the phase sequence although it causes a high-temperature shift of the SFM peak.

In order to clarify the nature of the SFM states attributed to our background susceptibility curves, we have measured the dc magnetization M vs H for fields $-4.5 \leq \mu_0 H \leq 4.5$ mT in steps of 0.1 mT (for $t = 1.3$ nm and $T = 220$ – 260 K also with enhanced resolution, 0.005 mT) at temperatures descending from 300 to 80 K ($t = 1.2$ nm) and 120 K ($t = 1.3$ nm), respectively. Each of the curves (partially shown in Fig. 4) was obtained after ZFC from 300 K.

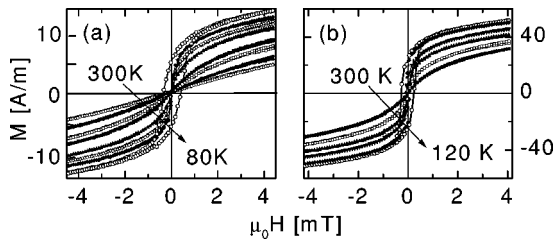


FIG. 4. Low-field magnetization curves M vs $\mu_0 H$ obtained on the DMIM with $t = 1.2$ (a) and 1.3 nm (b) after ZFC from 300 K to (a) $300, 260, 220, 180, 140, 120, 100, 80$ K and (b) $300, 260, 220, 180, 140,$ and 120 K, respectively.

Langevin-type SPM magnetization curves are encountered at high T until finite jumps, ΔM , occur at $H = 0$ upon cooling to below $T_c \approx 150$ ($t = 1.2$ nm) and 240 K ($t = 1.3$ nm), respectively. ΔM grows upon further cooling and signifies the stabilization of SFM ordering.²⁰

Obviously the SFM system behaves like a soft ferromagnet. Just below the respective T_c it is demagnetized in zero field and may be switched into its spontaneous values $\Delta M = \pm M_s$ by applying external fields in the order ± 0.1 mT. The quantity $(\Delta M/\Delta H)_{\max}$ vs T taken from the $M(H)$ curves²⁰ measures the linear susceptibility, $\chi'_1 = (dM/dH)_{\max}$, at $T > T_c$. It shows power-law-like behavior with a critical exponent $\gamma = 1.5 \pm 0.2$ in rough accordance with the 3D dipolar one, $\gamma = 1.69$.²¹ At $T < T_c$ it is roughly proportional to ΔM , which is a measure of M_s .

At lower temperatures, $T_f \approx 120$ and 190 K for $t = 1.2$ and 1.3 nm, respectively, the magnetization curves (Fig. 4) become hysteretic as evidenced by finite values of remanence M_r and coercive field H_c . Obviously the free-energy barrier due to the weak intraplanar anisotropy is no longer overcome by thermal activation, and both M_r and H_c increase upon further cooling to below T_f .²⁰ Since the T_f values roughly coincide with the onset of low- T dispersion in the ac susceptibility data [Figs. 2(c)–2(d)], it cannot be excluded that the observed hysteresis is related to the metastability of the reentrant SSG phase (see below). Indeed, we observe a weak time dependence of the hysteresis when varying the waiting time between individual data points, e.g., from $t_w \approx 90$ to 900 s. Changes of H_c of the $t = 1.3$ nm sample from 0.085 to 0.065 mT at $T = 150$ K may hint at some coupling of the hysteresis to the lossy dynamics of the SSG component as evidenced by its frequency dispersion (Fig. 2).

The appearance of the background signal hampers an exact evaluation of the reentrant glass transition for $t > 1.0$ nm. Nevertheless, the T dependence of the shoulders of $\chi'(f, T)$ in Figs. 2(b)–2(d) allows us to calculate glass temperatures $T_g \approx 60, 75,$ and 115 K, respectively, from the divergence of $1/(2\pi f)$ vs $T_m/T_g - 1$. Here, T_m refers to the “glassy component” after subtracting the SFM background approximated by $\chi'(f_{\max}, T)$, where $f_{\max} = 100$ Hz ($t = 1.1$ and 1.2 nm) and 500 Hz ($t = 1.3$ nm) [extended data set; not shown]), respectively. Figure 5 shows the tentative phase diagram, where $T_c(t)$ and $T_g(t)$ values define the SPM-SFM and SFM-RSSG (“reentrant superspin glass”) phase lines, respectively. The mean-field “phase line” $\Theta(t)$ lies slightly above $T_c(t)$, while the change from SSG to RSSG occurs at $t \approx t_0 = 1.05$ nm.

In order to understand the appearance of glassy freezing in the low- t limit and its gradual crossover into reentrant SFM behavior, various basic concepts have to be considered. First, collective freezing into a spin glasslike state requires frustration and disorder,¹³ conditions that are inherent to both dipolar interaction and random particle distribution. Second, the prevalence of FM correlations even in the glassy system ($t = 1.0$ nm) as evidenced by CW plots in Fig. 2 seems to be a peculiarity of dipolar systems. Qualitatively, it is a consequence of the energy gain of parallel polar alignments of the magnetic moments exceeding those of antiparallel equatorial

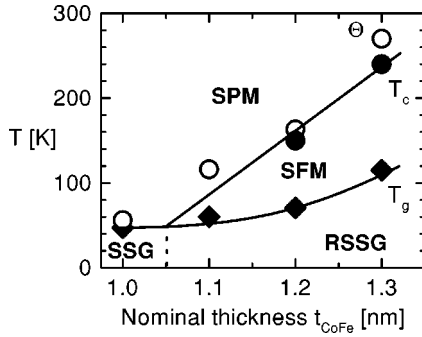


FIG. 5. Magnetic phase diagram of CoFe/Al₂O₃ DMIM's vs nominal CoFe thickness t showing interpolating phase lines SPM-SFM (T_c vs t) and SFM-RSSG (T_g vs t) together with Curie temperatures, Θ vs t , and the tentative vertical SSG-RSSG line (SPM=superparamagnetic, SFM=superferromagnetic, RSSG=reentrant superspin glass, and SSG=superspin glass).

ones. Empirically,⁶ the onset of ferromagnetism in parallel arrangements of linear nanomagnets critically depends on the intrachain distance. A similar “percolation limit” seems to exist in the random distribution of FM nanoparticles in DMIM's.¹⁰ Below this limit, one rather expects a glass transition at T_g with conventional¹³ concentration dependence as in dilute FM systems. This transition requires the average nearest-neighbor interaction $\langle J \rangle$ to be smaller than the width δJ of its distribution, where $k_B T_g \approx \delta J$. With growing t , the clearance between nearest-neighbor particles shrinks (assuming heterogeneous nucleation¹²), hence, δJ also grows. From the competition between growing $T_g(t)$ and $T_c(t)$, one expects the SFM regime to appear above some threshold value, $t=t_0$ for our DMIM's (Fig. 5).

Recently²² a comparative study of DMIM's with $t=0.9$ and 1.0 nm has shown that both of these samples show SSG properties with very similar values of T_g , τ_0 , $z\nu$, and γ . However, the order parameter exponents β obtained from a best-fitted dynamic scaling plot³ are markedly different. While $\beta \approx 1.0$ in the thin limit $t=0.9$ nm complies with conventional spin glass results,³ in the $t=1.0$ nm sample an unusually low value $\beta \approx 0.6$ seems to indicate some SFM clustering, hence, proximity to the SFM phase (Fig. 5).

Reentrance of a dipole glass phase (RDG) at low temperatures is a consequence of disorder. Analogously as proposed for reentrant amorphous ferromagnets,²³ a comparatively dense cluster (“percolating backbone”) first orders as a SFM network upon cooling to below T_c , while more dilute,

also percolating superspin clusters are freezing into random orientations only at $T_g < T_c$. The coexistence of SFM with RSSG order at low T does, hence, not invalidate thermodynamic principles, which require the SFM state at high T to possess larger entropy than the RSSG one at low T . This principle refutes the idea²⁴ that the reentrance might be due to blocking of superspins *within* the SFM subsystem. Besides, such a process would diminish rather than enhance (Fig. 2) the low- T susceptibility.

IV. CONCLUSION

In summary, our analysis clearly shows that both dipolar and FM “superexchange” interactions have to be taken into account in all of our DMIM systems. In the “low concentration” range, $t < t_0 \approx 1.05$ nm, dominant dipolar interaction gives rise to a SSG state at low T . At higher “concentrations,” $t > t_0$, “superexchange” interaction between close enough particles with finite size give rise to a virtually percolating SFM cluster and, hence, to a dispersionless susceptibility background, while the rest of the particles remains SPM, forming a SSG state at even lower T . Studies of this new phase and its reentrance properties (coexistence of states?²³) are presently underway.

The relevance of three-dimensionality in the ordering processes is yet unsettled. While the appearance of the SFM phase is in favor of 2D “superexchange” interaction (in case that it is of dipolar⁹ rather than of tunneling exchange²⁵ origin!), both the exponents $z\nu \approx 10$ and the low value of the quantity²⁶ $k = (1/T_m)(\Delta T_m / \Delta \log_{10} f) \approx 0.01$ of our glassy DMIM ($t=1.0$ nm) seems to hint at 3D rather than at 2D behavior. It will be particularly interesting to investigate DMIM's with $t=0.9$ nm (equidistant granule case; see above) in the *single* layer limit. In the SSG regime ($t < t_0$) ordering is expected only at $T_g=0$ by analogy with results on 2D Ruderman-Kittel-Kasuya-Yosida spin glasses like thin films of CuMn.²⁶

ACKNOWLEDGMENT

We gratefully acknowledge stimulating discussions with D. Fiorani, P. Nordblad, and D.G. Rancourt and valuable experimental help by M.M.P. de Azevedo and S. Sahoo. Thanks are due to DFG (Graduate School “Structure and Dynamics of Heterogeneous Systems”) and DAAD (Germany), and to CRUP and PRAXIS XXI (Portugal) for financial support.

¹J. L. Dormann, D. Fiorani, and E. Tronc, *J. Magn. Magn. Mater.* **202**, 251 (1999).

²L. Néel, *Ann. Geophys. (C.N.R.S.)* **5**, 99 (1949); W. F. Brown, Jr., *Phys. Rev.* **130**, 1677 (1963).

³C. Djurberg, P. Svedlindh, P. Nordblad, M. F. Hansen, F. Bødker, and S. Mørup, *Phys. Rev. Lett.* **79**, 5154 (1997); T. Jonsson, P. Svedlindh, and M. F. Hansen, *ibid.* **81**, 3976 (1998); P. Jönsson, P. Svedlindh, P. Nordblad, and M. F. Hansen, *cond-mat/0007464*, *J. Magn. Magn. Mater.* (to be published).

⁴J. L. Dormann, D. Fiorani, R. Cherkaoui, E. Tronc, F. Lucari, F. D’Orazio, L. Spinu, M. Nogues, H. Kachkachi, and J. P. Jolivet, *J. Magn. Magn. Mater.* **203**, 23 (1999).

⁵A. Sugawara, G. G. Hembree, and M. R. Scheinfein, *J. Appl. Phys.* **82**, 5662 (1997); J. Shen, R. Skomski, M. Klaua, H. Jeniches, S. Sundar Manoharan, and J. Kirschner, *Phys. Rev. B* **56**, 2340 (1997); C. Mathieu, C. Hartmann, M. Bauer, O. Buettner, S. Riedling, B. Roos, S. O. Demokritov, B. Hillebrands, B. Bartelien, C. Chappert, D. Decanini, F. Rousseaux, E. Cambrial, A.

- Müller, B. Hoffmann, and U. Hartmann, *Appl. Phys. Lett.* **70**, 2912 (1997); J. Hauschild, H. J. Elmers, and U. Gradmann, *Phys. Rev. B* **57**, R677 (1998).
- ⁶R. P. Cowburn, A. O. Adeyeye, and M. E. Welland, *New J. Phys.* **1**, 16.1 (1999).
- ⁷M. R. Scheinfein, K. E. Schmidt, K. R. Heim, and G. G. Hembree, *Phys. Rev. Lett.* **76**, 1541 (1996).
- ⁸J. M. Luttinger and L. Tisza, *Phys. Rev.* **70**, 954 (1946); P. N. Vorontsov-Vel'yaminov and I. A. Favorskii, *Fiz. Tverd. Tela (Leningrad)* **15**, 1298 (1974) [*Sov. Phys. Solid State* **15**, 1937 (1974)]; R. Kretschmer and K. Binder, *Z. Phys. B* **34**, 375 (1979).
- ⁹Yu. G. Pogorelov, G. N. Kakazei, M. M. Pereira de Azevedo, and J. B. Sousa, *J. Magn. Magn. Mater.* **196–197**, 112 (1999); Yu. G. Pogorelov, *IEEE Trans. Magn.* (to be published).
- ¹⁰W. Kleemann, Ch. Binek, O. Petravic, G. N. Kakazei, Yu. G. Pogorelov, J. B. Sousa, M. M. Pereira de Azevedo, S. Cardoso, and P. P. Freitas, *J. Magn. Magn. Mater.* (unpublished).
- ¹¹L. F. Schelp, A. Fert, F. Fettar, P. Holody, S. F. Lee, J. L. Maurice, F. Petroff, and A. Vaures, *Phys. Rev. B* **56**, R5747 (1997); S. Sankar, B. Dieny, and A. E. Berkowitz, *J. Appl. Phys.* **81**, 5512 (1997); B. Dieny, S. Sankar, M. R. McCartney, D. J. Smith, P. Bayle-Guillemaud, and A. E. Berkowitz, *J. Magn. Magn. Mater.* **185**, 283 (1997); S. Sankar, A. E. Berkowitz, and D. J. Smith, *Appl. Phys. Lett.* **73**, 535 (1998).
- ¹²G. N. Kakazei, P. P. Freitas, S. Cardoso, A. M. L. Lopes, M. M. Pereira de Azevedo, Yu. G. Pogorelov, and J. B. Sousa, *IEEE Trans. Magn.* **35**, 2895 (1999).
- ¹³K. H. Fischer and J. A. Hertz, *Spin Glasses* (Cambridge University, Cambridge, 1991); J. A. Mydosh, *Spin Glasses: An Experimental Introduction* (Taylor and Francis, London, 1993).
- ¹⁴E. Bonetti, L. Del Bianco, D. Fiorani, D. Rinaldi, R. Caciuffo, and A. Hernando, *Phys. Rev. Lett.* **83**, 2829 (1999).
- ¹⁵G. N. Kakazei, Yu. G. Pogorelov, A. M. L. Lopes, J. B. Sousa, S. Cardoso, P. P. Freitas, M. M. Pereira de Azevedo, and E. Snoeck, *J. Appl. Phys.* (unpublished).
- ¹⁶K. Gunnarsson, P. Svedlindh, P. Nordblad, P. Lundgren, H. Aruga, and A. Ito, *Phys. Rev. Lett.* **61**, 754 (1988).
- ¹⁷H.-D. Pfannes, A. Mijovilovich, R. Magalhães-Paniago, and R. Paniago, *Phys. Rev. B* **62**, 3372 (2000).
- ¹⁸K. Gunnarsson, P. Svedlindh, P. Nordblad, P. Lundgren, H. Aruga, and A. Ito, *Phys. Rev. B* **43**, 8199 (1991).
- ¹⁹G. A. Takzei, I. Mirebeau, L. P. Gun'ko, I. I. Sych, O. B. Surzhenko, S. V. Cherepov, and Yu. N. Troschenkov, *J. Magn. Magn. Mater.* **202**, 376 (1999).
- ²⁰O. Petravic (unpublished).
- ²¹M. E. Fisher and A. Aharony, *Phys. Rev. Lett.* **30**, 559 (1973).
- ²²O. Petravic, W. Kleemann, Ch. Binek, G. N. Kakazei, Yu. G. Pogorelov, J. B. Sousa, S. Cardoso, and P. P. Freitas, *Phase Transit.* (to be published).
- ²³B. R. Coles, B. V. B. Sarkissian, and R. H. Taylor, *Philos. Mag. B* **37**, 489 (1978); S. N. Kaul and S. Srinath, *J. Phys.: Condens. Matter* **10**, 11 067 (1998); S. Srinath and S. N. Kaul, *Europhys. Lett.* **51**, 441 (2000).
- ²⁴D. G. Rancourt (private communication).
- ²⁵V. N. Kondratyev and H. O. Lutz, *Phys. Rev. Lett.* **81**, 4508 (1998); *Eur. Phys. J. D* **9**, 483 (1999).
- ²⁶L. Sandlund, P. Granberg, L. Lundgren, P. Nordblad, P. Svedlindh, J. A. Cowen, and G. G. Kenning, *Phys. Rev. B* **40**, 869 (1989); P. Granberg, J. Mattsson, P. Nordblad, L. Lundgren, R. Stubi, J. Bass, D. L. Leslie-Pelecki, and J. A. Cowen, *ibid.* **44**, 4410 (1991).